Automatic Extraction of Field Boundaries from Aerial Imagery

Matthias Butenuth, Bernd-Michael Straub, and Christian Heipke

Institute of Photogrammetry and GeoInformation, University of Hannover,
Nienburger Str.1, D-30167 Hannover, Germany
{butenuth, straub, heipke}@ipi.uni-hannover.de

Abstract. In this paper work on automatic image analysis methods extracting field boundaries from aerial imagery is presented. The fields respectively their surrounding boundaries are described together with additional GIS-data in an integrated semantic model to get an overview of the different characteristics and how to exploit the prior knowledge. The image analysis strategy is derived from the semantic model taking into account an automatic processing flow. First a watershed segmentation is carried out with a subsequent grouping of the resulting basins. Potential field areas are divided, if necessary, in smaller and more detailed fields using a line extraction and additionally introduced prior GIS-knowledge. The resulting preliminary boundaries are in some part geometrically inaccurate, which is why a snake algorithm is initialized to refine the geometrical correctness. The results of the different steps demonstrate the potential of the proposed solution.

1 Introduction and Motivation

In this paper work on automatic extraction of field boundaries from aerial imagery is described. Field boundaries become more and more important: One application area is the derivation of potential wind erosion risk fields for geo-scientific questions, which can be generated with additional input information about the prevailing wind direction, wind shelters and soil parameters, as described in [18]. Another area is the agricultural sector, where information about field geometry is important for tasks concerning precision farming or the monitoring of subsidies [1], [9].

In the past, several investigations have been carried out regarding the automatic extraction of man-made objects such as buildings or roads, see for example [4] and [13]. Similarly, investigations regarding the extraction of trees have been accomplished, see [10] for an overview of approaches suitable for woodland and [17] for a method to extract trees not only capable for woodland but also in the open landscape.

In contrary, the extraction of field boundaries from high resolution imagery is still not in an advanced phase: [12] presented an approach to update and refine topologically correct field boundaries by a fusion of raster-images and vector-map data. Focusing on the reconstruction of the geometry and features of the land-use units, the acquisition of new field boundaries is not discussed. In [19] a so called

region competition approach is described, which extracts field boundaries from aerial images with a combination of region growing techniques and snakes. To initialize the process, seed regions have to be defined manually, which is a time and cost-intensive procedure. In [2] a technique for predicting missing field boundaries from satellite images is presented, using a comparison of modal land cover and local variance. The approach involves manual post processing, because only fields with a high likelihood of missing boundaries are identified, not field boundaries directly. The aim of the solution, presented in this paper, is a fully automatic extraction of field boundaries from high resolution aerial CIR-imagery. Consequently, the proposed strategy differs from the mentioned approaches.

In general, the recognition of objects with the help of image analysis methods starts often with an integrated modelling of the objects of interest and the surrounding scene. Furthermore, exploiting the context relations between different objects leads to more overall and holistic descriptions, see for example [5] and [8]. The use of prior knowledge (e.g. GIS-data) supporting object extraction can lead to better results as shown in [3] and [6]. These aspects are incorporated in the model for the extraction of field boundaries and are reflected in the resulting strategy.

Initially, the integration of GIS-data and imagery in one semantic model is briefly described in the next section to obtain an overview of the numerous relations between the objects to be extracted and the prior knowledge. Afterwards, the strategy and approach to extract field boundaries is explained, followed by results to demonstrate the potential of the proposed solution. Finally, further work required is discussed in the conclusions.

2 Semantic Model for the Integration of GIS-Data and Aerial Imagery

Describing the integration of GIS-data and aerial CIR-imagery in one semantic model is the starting point for successful object extraction, as highlighted in detail in [7]. The semantic model is differentiated in an object layer, consisting of the real world, a GIS-layer, a geometric and material part, as well as an image layer (cf. Fig. 1). The model is based on the assumption, that the used CIR-images are generated in summer, when the vegetation is in an advanced period of growth.

The use of prior knowledge plays an important role, which is represented in the semantic model with an additional GIS-layer. Vector data of the ATKIS DLMBasis (German Authoritative Topographic-Cartographic Information System) is used, which is an object based digital landscape model of the whole country: (1) Field boundaries are exclusively located in the open landscape, thus, further investigations are focused to this area. The open landscape is not directly modelled in the ATKIS DLMBasis, this is why this information has to be derived by selecting all areas, which are not settlements, forests or water bodies. (2) The road network, rivers and railways can be used within the open landscape as prior knowledge: The geometries of these GIS-objects are introduced in the semantic model with a direct relation from the GIS-layer to the real world (cf. Fig. 1): For example the ATKIS-objects 3101 (roads) and 3102 (paths) are linked to the road segments of the real world and, thus, usable as field

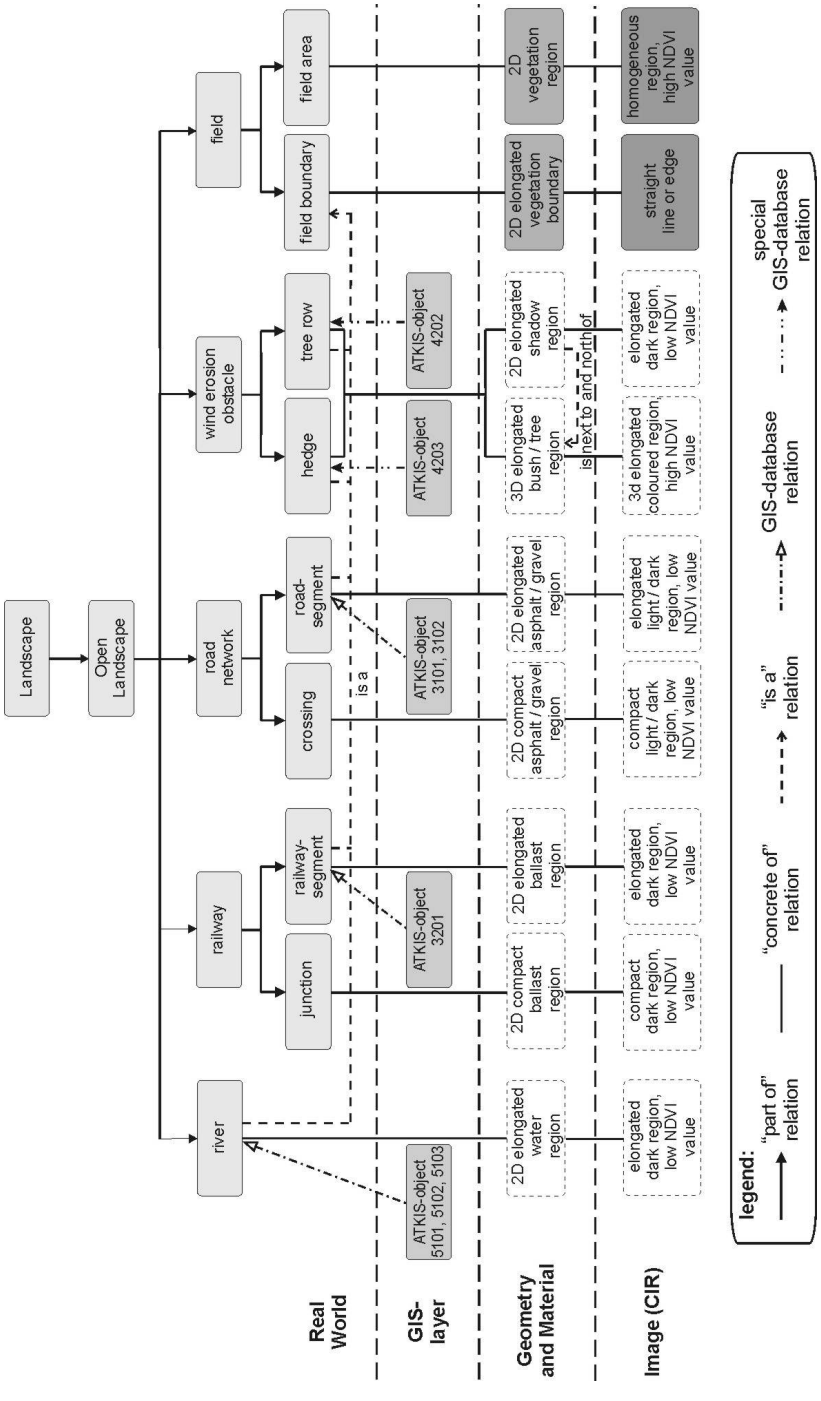

Fig. 1. Semantic Model

boundaries (e.g. a road is a field boundary). (3) Tree rows and hedges are only captured in the ATKIS-data, if they are longer than 200 m and lies along roads or are formative for the landscape, therefore, the relation from the GIS-layer to the real world is limited. The modelling of all GIS-objects in the geometry and material layer together with the image layer is not of interest, because they do not have to be extracted from the imagery (depicted with dashed lines in Fig. 1).

The object to be extracted, the *field*, is divided in the semantic model in *field area* and *field boundary* in order to allows for different modelling in the layers (cf. Fig. 1 on the right side): The field area is a 2D vegetation region, which is a homogeneous region with a high NDVI (Normalized Difference Vegetation Index) value in the CIR-image. The field boundary is a 2D elongated vegetation boundary, which is formed as a straight line or edge in the image. Both descriptions lead to the desired result from different sides.

3 Strategy to Extract Field Boundaries

3.1 General Strategy

The general strategy for the extraction of field boundaries is derived from the modelled characteristics of the fields and their surrounding boundaries taking into account the realization of an automatic process flow (cf. Fig. 2). Aerial CIR-images and GIS-data are the input data to initialize the flowchart: Initially, the open landscape is derived from the GIS-data taking into account the modelled constraints (cf. section 2). In addition, within the open landscape, *regions of interest* are selected using the road network, rivers, railways, tree rows and hedges as borderlines in order to handle the large datasets in an appropriate manner (cf. Fig. 5 for an example of a selected region of interest). Consequently, the borderlines of the regions of interest are field boundaries, which are already fixed, and the image analysis methods are focused to the field boundaries within the regions of interest. The homogeneity of the vegetation within each field enables a segmentation of field areas, processed in a coarse scale to ignore small disturbing structures. Identical vegetation of neighbouring fields leads to missing field boundaries, which can be derived by a line extraction in a finer scale. Further knowledge will be introduced at this time to exploit GIS-data, which gives evidence of field boundaries *within* the selected regions of interest (e.g. dead-end streets or tree rows). The derived preliminary field boundaries are in some parts inaccurate and a snake algorithm is initialized to refine their geometric accuracy.

3.2 Segmentation of Potential Field Areas

In each region of interest a segmentation is carried out to exploit the modelled similar characteristics and homogeneity of each field. As data source the red channel of the CIR-images is used, which according to our experience fulfils the homogeneity criterion best. To utilize the changing vegetation from one field to the next, the

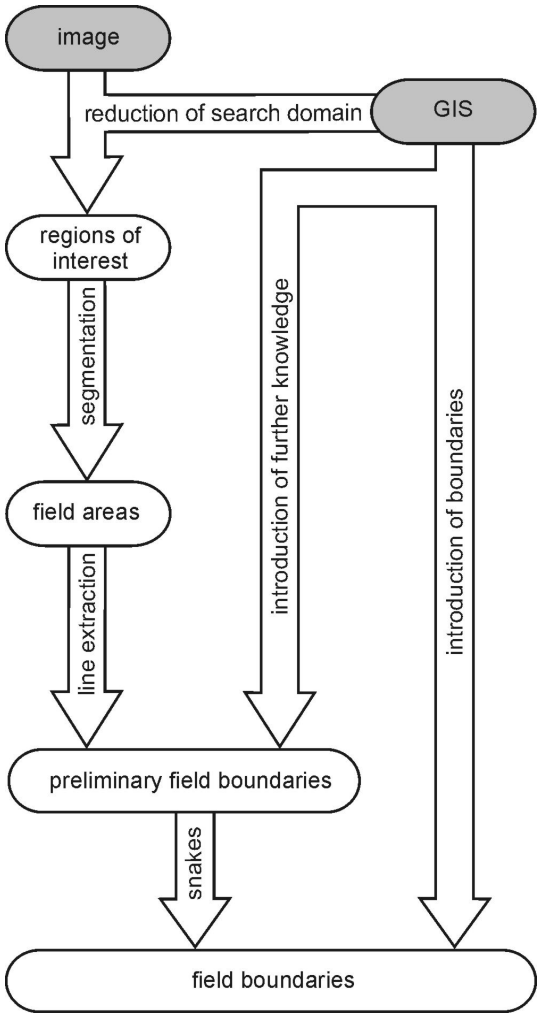

Fig. 2. Flowchart of the strategy

absolute values of the gradient are computed. The topography of the grey values is used to accomplish a *watershed segmentation* [14]. The resulting basins are marked with their corresponding mean grey value in the red channel. Potential field areas are derived grouping the basins, if they lie next to each other and have a low grey value difference, additionally considering a minimum size (cf. Fig. 6, each grey value is one segmented field area).

3.3 Deriving Missing Field Boundaries by Line Extraction and Grouping

The field areas obtained from the segmentation step are only intermediate results. The reason is, that the case of identical vegetation in neighbouring fields – and therefore a

missing boundary – is not taken into account. Accordingly, a *line extraction* [15] is carried out within each field area to derive missing field boundaries. The extracted short pieces of lines are grouped to straight long lines in consideration of a minimum length due to the characteristics of the field boundaries. In addition, intersection points of the lines are calculated, if the end points of the corresponding lines have a minimum distance in between. Furthermore, the lines are extended to the boundaries of the field areas, if the distance lies again below a threshold. Results of the extracted lines are depicted in Fig. 6 in white.

Further GIS knowledge referring to fixed field boundaries *within* the regions of interest (e.g. dead-end streets or tree rows) is introduced to support the extraction of field boundaries (cf. Fig. 2, in Fig. 6 the lines are depicted in black). The preliminary field areas are split by the extracted or additionally introduced lines yielding the preliminary field boundaries (cf. Fig 7, boundaries of the fields are depicted in black).

4 Using Snakes to Improve the Geometric Quality of the Results

The preliminary field boundaries are in some part geometrically inaccurate, which is why a classical *snake* algorithm is used to perform the precise delineation. To initialize the processing, a smallest bounding rectangle of each generated field is calculated, because most fields are four corned polygons and this knowledge can be exploited by using the initial information about the corners of the rectangles as well as the straight boundaries at the sides.

Snakes were originally introduced in [11] as a mid-level algorithm which combines geometric and/or topologic constraints with the extraction of low-level features from images. The principal idea is to define a contour with the help of mechanical properties like elasticity and rigidity (internal energy), to initialize this contour close to the boundary of the object one is looking for. In Fig. 3 an example is shown: The preliminary result of the field boundary is used to initialize the snake (depicted in white) and furthermore the processed different iteration steps are depicted to show the movement of the snake (depicted in black). The contour can be looked upon as a virtual rubber cord which can be used to detect valleys in a hilly landscape with the help of gravity. If the snake is initialized close enough to the valleys of the landscape, the gravity drags it into the valleys. The "landscape" may be a surface model, an image, or the edges of an image. The movement originates in a field of gradients, which can be computed on the base of an edge detector's result.

The whole energy of the snake E_{snake}, to be minimized, is the sum of the internal energy $E_{v(s,\,t)}$ and the external energy E_{ext}. The definition of the internal and external energy is given in [11]. The internal energy is described in the following in detail due to the speciality of the presented work, given in equation (1):

$$E_{v(s,t)} = \tfrac{1}{2}\left(\alpha(s)\cdot\left|v'(s,t)\right|^2 + \beta(s)\cdot\left|v''(s,t)\right|^2\right) \qquad (1)$$

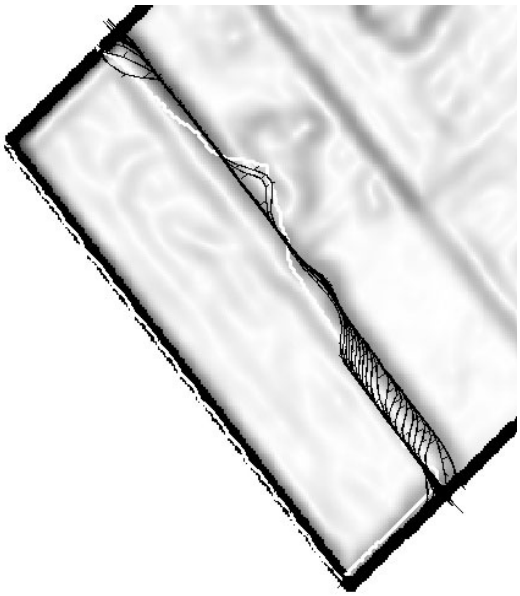

Fig. 3. Example for the measurement of the outline with a snake: Initialization is depicted in white, different optimization steps are depicted in black

The application *field boundaries* leads to a possibility to select special weight functions *α(s) and β(s)*, which are used to control the elasticity and rigidly of the contour *v(s,t)*; *s* is the arc length and *t* the iteration number. The weight functions are depicted in Fig. 4: At the corners of a rectangle with a width *a* and a height of *b*, *α(s)* obtains a high weight and *β(s)* a low weight, and along the edges between the corners *α(s)* is chosen low and *β(s)* high. This leads to stiff edges along the expected straight lines of the field and allows the snake to form four corners.

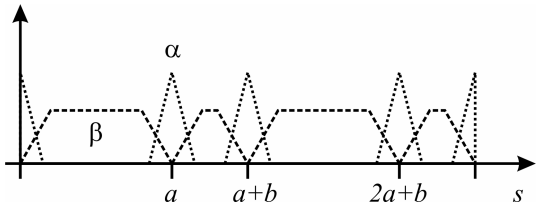

Fig. 4. Control function for the parameters *α* and *β* against the way *s* , *a* is the width and *b* the height of a rectangle used for the initialization of the snake

As external force the absolute values of the gradients of the given red channel of the imagery are used. Additionally, the boundaries of the region of interest are manipulated to form "deep valleys" to steer the snake to this fixed boundaries (cf. section 3). In order to enhance the radius of convergence of the snake, the sum of the gradients absolute values over six scale levels with a $\sigma = 1, 2, 4 \ldots 32$ is used, as proposed in [16].

5 Results

In this section example results from an application area are presented. In Fig. 5 the red channel of the imagery of a selected region of interest is depicted, the boundaries of the region have been derived from the ATKIS-data. The preliminary results of the segmentation are shown in Fig. 6, superimposed with extracted lines in white and additional further information from the GIS-data in black. The final result of the segmentation step is depicted in Fig. 7. It must be recognized, that the geometric correctness is not always satisfying: For example, the field boundaries in the middle top of the depicted region of interest in Fig. 7 are not exactly identical to the real boundaries of the fields in the image. The initialized snake algorithm is a reasonable possibility to refine these preliminary results, details for one field and the associated iteration steps of the snake algorithm are highlighted in Fig. 3. The refined result of the extraction of field boundaries is depicted in Fig. 8. The geometric correctness has improved, but the topological correctness has in some parts suffered.

6 Conclusions

In this paper work on the automatic extraction of field boundaries from aerial imagery is presented. An integrated semantic model and a subsequently derived strategy of different steps is proposed exploiting the modelled characteristics of the objects of interest. The segmentation of field areas based on the gradients in coarse scale of the imagery is carried out using a watershed segmentation. In the future, the use of colour and/or texture may stabilize the segmentation step. Extracted and grouped lines with different criteria in a finer scale and additional introduced prior knowledge from GIS-data are used to split the segments in detailed and improved preliminary results. Finally, the derived field boundaries are geometrically refined using snakes. The results demonstrate the potential of the proposed solution. Future work will be devoted to the development of an integrated network of snakes for all field areas of the region of interest together, not only a snake initialization for each field separately, in order to improve the topological correctness.

Acknowledgements

Parts of this work are funded in the programme GEOTECHNOLOGIEN by the Federal Ministry for Education and Research (BMBF) and the German Research Council (DFG) with the publication no. GEOTECH-70.

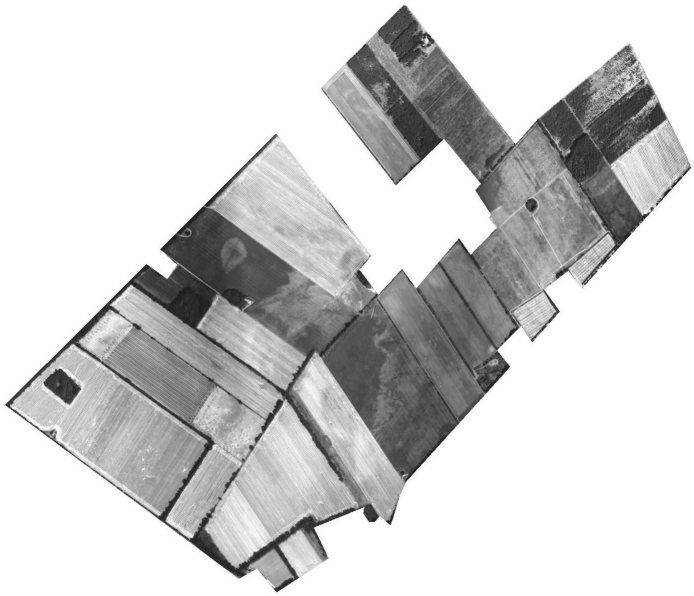

Fig. 5. Selected region of interest, depicted is the red channel of the aerial image

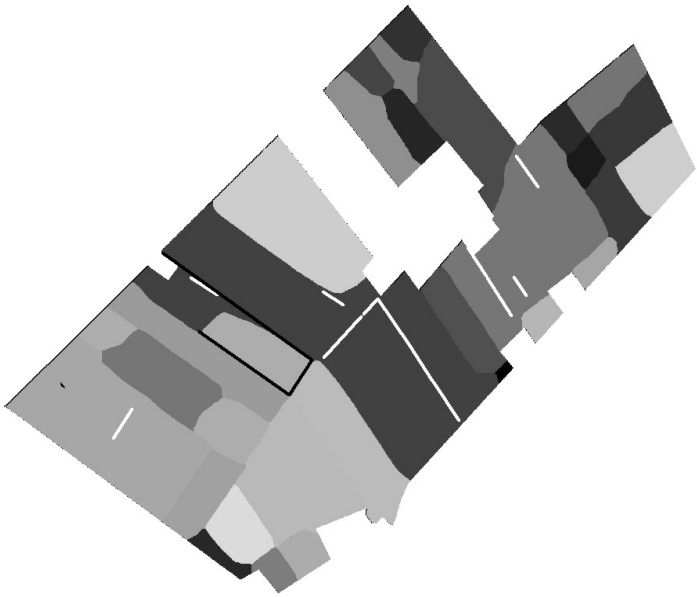

Fig. 6. Preliminary segmentation result, additionally superimposed with extracted lines (white) and further prior knowledge (black)

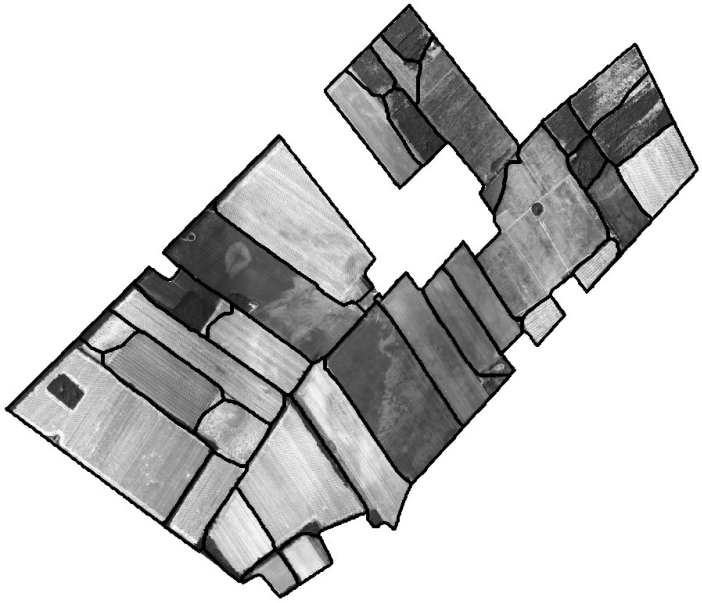

Fig. 7. Result of the preliminary field boundary extraction is depicted in black

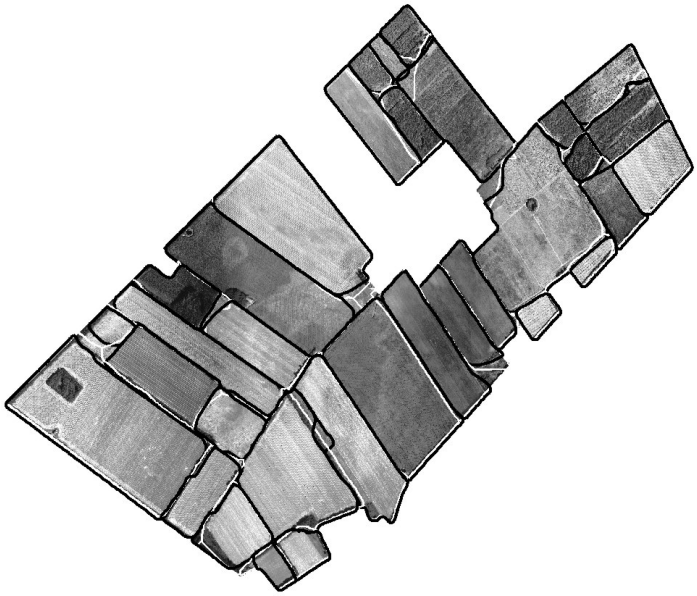

Fig. 8. Refined result of the field boundaries after the snake-processing: Initialization is depicted in white, field boundaries are depicted in black

References

1. Anderson, J. E., Fischer, R. L., Deloach, S. R.: Remote Sensing and Precision Agriculture: Ready for Harvest or Still Maturing?. Photogrammetric Engineering & Remote Sensing, Vol. 65, No. 10 (1999) 1118-1123
2. Aplin, P., Atkinson, P. M.: Predicting Missing Field Boundaries to Increase Per-Field Classification Accuracy. Photogrammetric Engineering & Remote Sensing, Vol. 70, No. 1 (2004) 141-149
3. Baltsavias, E. P.: Object Extraction and Revision by Image Analysis Using Existing Geodata and Knowledge: Current Status and Steps towards Operational Systems. ISPRS Journal of Photogrammetry and Remote Sensing, Vol. 58, No. 3-4 (2004) 129-151
4. Baltsavias, M., Gruen, A., Van Gool, L. (eds.): Automatic Extraction of Man-Made Objects from Aerial and Space Images III. A.A. Balkema Publishers, Lisse Abingdon Exton(PA) Tokio (2001)
5. Baumgartner, A., Eckstein, W., Mayer, H., Heipke, C., Ebner, H.: Context Supported Road Extraction. Gruen Baltsavias Henricson (eds), Automatic Extraction of Man-Made Objects from Aerial and Space Images II, Birkhäuser, Basel Boston Berlin, Vol. 2, (1997) 299-308
6. Bordes, G., Guérin, P., Maitre, H.: Contribution of External Data to Aerial Image Analysis. International Archives of Photogrammetry, Remote Sensing and Spatial Information Sciences, Vol. XXXI, No. B4/IV (1996) 134-138
7. Butenuth, M., Heipke, C.: Integrating Imagery and ATKIS-data to Extract Field Boundaries and Wind Erosion Obstacles. Geotechnologien Science Report "Information Systems in Earth Management", No. 4, Koordinierungsbüro Geotechnologien, Potsdam, (2004) 40-44
8. Butenuth, M., Straub, B.-M., Heipke, C., Willrich, F.: Tree Supported Road Extraction from Aerial Images Using Global and Local Context Knowledge. Crowley Piater Vincze Paletta (eds), Lecture Notes in Computer Science, Springer Verlag, Graz, Austria, Vol. LNCS 2626, (2003) 162-171
9. Grenzdörffer, G.: Konzeption, Entwicklung und Erprobung eines digitalen integrierten flugzeuggetragenen Fernerkundungssystems für Precision Farming (PFIFF). Dissertation Reihe C, Deutsche Geodätische Kommission, München, No. 552 (2002)
10. Hill, D. A., Leckie, D. G. (eds.): International forum: Automated interpretation of high spatial resolution digital imagery for forestry, February 10-12, 1998. Natural Resources Canada, Canadian Forest Service, Pacific Forestry Centre, Victoria, British Columbia (1999)
11. Kass, M., Witkin, A., Terzopoulus, D.: Snakes: Active Contour Models. International Journal of Computer Vision, Vol. 1, (1988) 321-331
12. Löcherbach, T.: Fusing Raster- and Vector-Data with Applications to Land-Use Mapping. Inaugural-Dissertation der Hohen Landwirtschaftlichen Fakultät der Universität Bonn, Bonn, (1998)
13. Mayer, H.: Automatische Objektextraktion aus digitalen Luftbildern. Habilitation Reihe C, Deutsche Geodätische Kommission, München, No. 494 (1998)
14. Soille, P. (ed.): Morphological Image Analysis: Principles and Applications. Springer, Berlin Heidelberg NewYork (1999)
15. Steger, C.: An unbiased detector of curvilinear structures. IEEE Transactions on Pattern Analysis and Machine Intelligence, Vol. 20, No. 2 (1998) 311-326
16. Straub, B.-M.: Automatic Extraction of Trees from Aerial Images and Surface Models. Ebner Heipke Mayer Pakzad (eds), The International Archives of the Photogrammetry, Remote Sensing and Spatial Information Sciences, ISPRS, München, Germany, Vol. XXXIV, Part 3/W8, (2003) 157-164
17. Straub, B.-M.: Automatische Extraktion von Bäumen aus Fernerkundungsdaten. Dissertation Reihe C, Deutsche Geodätische Kommission, München, No. 572 (2003)

18. Thiermann, A., Sbresny, J., Schäfer, W.: GIS in WEELS - Wind Erosion on Light Soils. GeoInformatics, No. 5 (2002) 30-33
19. Torre, M., Radeva, P.: Agricultural Field Extraction from Aerial Images Using a Region Competition Algorithm. International Archives of Photogrammetry and Remote Sensing, Amsterdam, Vol. XXXIII, No. B2 (2000) 889-896